## XFEM Simulation of Functionally Graded Plates with Arbitrary Openings

## Huu -Dien Nguyen\*



Use your smartphone to scan this QR code and download this article

Long An University of Economics and Industry, Vietnam

#### Correspondence

**Huu -Dien Nguyen**, Long An University of Economics and Industry, Vietnam

Email:

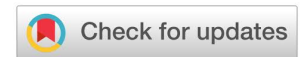
nguyen.dien@daihoclongan.edu.vn

#### History

Received: 09-05-2025Revised: 08-09-2025Accepted: 18-08-2005Published Online: 03-11-2025

#### DOI:

https://doi.org/10.32508/stdj.v28i4.4484



#### Copyright

© VNUHCM Press. This is an openaccess article distributed under the terms of the Creative Commons Attribution 4.0 International license.



#### **ABSTRACT**

The present article addresses the impact of arbitrary-shaped holes in plates composed of functionally graded materials (FGMs). A modeling strategy is developed that avoids the need for remeshing around internal hole boundaries. The numerical formulation combines the level set method with the extended finite element method (X-FEM), where the finite element approximation is enhanced by enrichment functions through the partition of unity framework. The level set approach is employed to accurately capture complex hole geometries. Numerical case studies demonstrate the precision and robustness of the proposed methodology, showing that the discrepancies in displacement and stress concentration factor between the proposed and reference methods are below 1.3%, thereby confirming the accuracy of the model.

**Key words:** XFEM, Level set method, holes, FGM

## INTRODUCTION

Functionally graded materials (FGMs) have found widespread applications in engineering fields such as aerospace structures, marine engineering, nuclear reactors, and biomedical implants, owing to their ability to tailor material properties for enhanced thermal resistance, mechanical performance, and durability. In many of these applications, structural components are designed with openings for functional purposes, such as weight reduction, ventilation, access to internal parts, or integration with other systems. However, the presence of openings can significantly alter the stress distribution and displacement fields, potentially leading to stress concentration and reduced load-bearing capacity. For FGM plates, these effects are further complicated by the spatial variation of material properties, making accurate modeling and analysis essential for safe and efficient design. Therefore, understanding and predicting the mechanical behavior of FGM plates with arbitrary openings is of practical importance to ensure performance reliability in demanding engineering environments 1,2.

The XFEM is a prominent method employed for simulating structures exhibiting discontinuities or singularities. Its principal benefit lies in modeling discontinuities independently of the mesh, overcoming a key difficulty encountered in standard finite element methods. By introducing localized enrichments to the approximation space, XFEM significantly extends the capabilities of the conventional FEM. This method

finds widespread applications, including in the simulation of crack growth, material interfaces, and void-containing structures<sup>3</sup>.

The novelty of the present work lies in the development of an XFEM-level set framework specifically tailored for functionally graded plates with arbitrary-shaped openings, eliminating the need for remeshing around complex boundaries. Unlike most existing studies, which focus on isotropic materials, regular hole shapes, or require mesh adaptation, our method:

- Combines the level set method with absolute enrichment functions to accurately capture arbitrary geometries in FGMs.
- 2. Avoids remeshing, thus reducing computational cost while maintaining high accuracy.
- Validates the approach through comparison with the robust meshfree EFG method, showing excellent agreement (<1.3% error) even for challenging geometries like elliptical openings.

## **RESEARCH METHOD**

#### Level set method

The level set method, which is a numerical method for tracking interfaces and shapes, is usually used in the XFEM to capture the discontinuities. In two dimensions, a close curve  $r^{int}$  can be represented as the zero-level set of a function  $\varphi$  as follows <sup>4–6</sup>:

$$\Gamma = \{x \in \mathbb{R}^2 : \phi(x) = 0\}$$
 (2.1)

The function  $\phi$ , known as the level set function, is typically positive inside the domain enclosed by the curve

Cite this article: Nguyen H D. XFEM Simulation of Functionally Graded Plates with Arbitrary Openings. Sci. Tech. Dev. J. 2025; 28(4):3870-3877.

 $r^{int}$ , and negative outside it. This formulation enables an implicit representation of the interface  $r^{int}$  through  $\phi$ . One notable instance of a level set function is the signed distance function.

$$\phi(x) = \mp \min_{x_{\Gamma} \in \Gamma} \|x - x_{\Gamma}\| \quad (2.2)$$

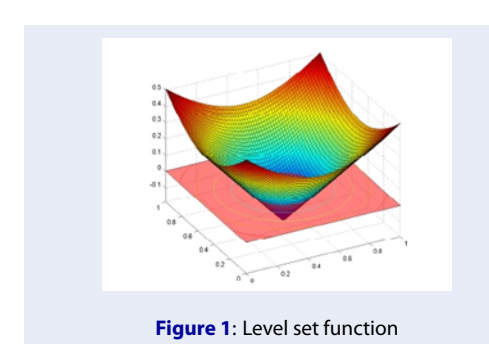
If the void or inclusion has a circular shape, the corresponding level set function  $\phi$  is defined as:

$$\phi = ||x - x_c|| - r_c$$
 (2.3)

Here,  $x_c$  and  $r_c$  represent the center and radius of the circular void or inclusion. An illustration of a level set function for a circular shape is provided in Figure 1 . In cases involving multiple discontinuities, the level set function at any location is determined by taking the minimum value among all level set functions representing the individual features.

## **General formulation**

In XFEM, enrichment functions are used to account for discontinuities in regions surrounding them. Let us consider a 2D domain  $\Omega \subset \mathbb{R}^2$ , divided into  $N^{el}$  finite elements. Denote I as the complete set of nodes in the mesh, and J as the subset of nodes that need enrichment. The displacement field can then be expressed in the general form shown below  $^{7-11}$ .



Equation (2.4) represents the general form of the displacement field u(x) in the extended finite element framework. In this formulation, u(x) is expressed as the sum of the standard finite element approximation and an enrichment part that accounts for discontinuities or singularities:

$$u(x) = \underbrace{\sum_{i \in I} N_i(x) u_i}_{std.FE.approx.} + \underbrace{\sum_{j \in J} M_J(x) \psi_j a_j}_{inrichment} (2.4)$$

where  $N_i(x)$  are the standard finite element shape functions associated with nodal displacements  $u_i$ ,  $M_j(x)$ ,  $\psi_j$  are the shape functions for the enriched nodes, are the enrichment functions, and  $a_j$  are the additional degrees of freedom introduced by the enrichment. The first term represents the standard finite element (FE) approximation, while

the second term introduces the enrichment that enables the model to capture features such as cracks, holes, or material interfaces without remeshing.

This clarification has been added to the manuscript before Equation (2.4) to explicitly define the displacement field.

In this study, the "absolute enrichment function"  $\psi$  refers to the absolute value level set enrichment, defined as:

$$\psi(x) = |\phi(x)|$$

where  $\phi(x)$  is the signed distance function obtained from the level set representation of the hole boundary. This enrichment captures the discontinuity in the gradient of the displacement field across the interface while maintaining displacement continuity. The absolute value is used instead of the sign function to ensure a smooth transition and avoid introducing displacement jumps that are not physically present in the problem under consideration.

In this formulation, the first term is the same as the standard FEM approximation, while the second term accounts for the enrichment.  $N_i$  are the usual shape functions used in FEM, and  $u_i$  are the unknown nodal displacements. The enrichment is introduced through functions  $\psi_j$ , with corresponding unknown coefficients  $a_j$ . The functions  $M_j$  also serve as shape functions, and although they might differ from  $N_j$ , they are required to form a partition of unity—for example:

$$\sum_{j\in J} M_j = 1 \quad (2.5)$$

Equation (2.4) can be seamlessly integrated into the classical finite element formulation by interpreting the enriched unknowns  $a_j$  as extra degrees of freedom associated with enriched nodes. Similar to standard FEM procedures, the solution seeks a displacement field u that minimizes the total potential energy, in accordance with the variational principle:

$$\Pi = \frac{1}{2} \int_{\Omega} \in^{T} C \in d\Omega - \int_{\Gamma} u^{T} T d\Gamma$$
 (2.6)

Here,  $\in$  refers to the strain tensor, C is the elasticity (stiffness) matrix of the material, and T indicates the boundary tractions applied on the prescribed edges. The strain expressions are obtained by differentiating the displacement approximation given in Equation (2.4), as shown below:

$$\in = Bd$$
 (2.7)

The vector d denotes the extended set of nodal displacements, incorporating both standard degrees of freedom and enriched unknowns  $a_j$ . The corresponding strain–displacement matrix B is formulated in the following manner:

$$B_{i} = \begin{bmatrix} N_{i,x} & 0 & (M_{i}\psi_{i})_{,x} & 0\\ 0 & N_{i,y} & 0 & (M_{i}\psi_{i})_{,y}\\ N_{i,y} & N_{i,x} & (M_{i}\psi_{i})_{,y} & (M_{i}\psi_{i})_{,x} \end{bmatrix} (2.8)$$

For nodes that are not enriched, the formulation of the B matrix is the same as in standard finite element analysis. Substituting Equations (2.4) and (2.7) into Equation (2.6) leads to:

$$\Pi = \frac{1}{2}d^TKd - d^TF \quad (2.9)$$

where

$$K_{ij} = \int_{\Omega} B_i^T C B_j d\Omega$$

$$F_i = \int_{\Gamma} B^{\mathbf{T}} T d\Gamma$$

where  $P_i \equiv N_i$  for a non-enriched node, and  $P_i \equiv M_i \psi_i$  for an enriched node.

Applying the condition of stationary potential energy from Equation (2.9) results in the standard form of the equilibrium equation:

$$Kd = F$$
 (2.10)

## **Implementation**

A key difficulty in XFEM implementation lies in calculating the stiffness matrix integrals for enriched elements. For each enriched element, it is crucial to identify the points where the zero-level set intersects the edges of the element, if present. The element is then subdivided into smaller triangles at these zero-level set points using Delaunay triangulation, and Gaussian integration is applied to each sub-triangle. Since only absolute enrichment functions are used, a third-order integration is adequate. The integration process is shown in Figure 2 <sup>12</sup> <sup>13-15</sup>.

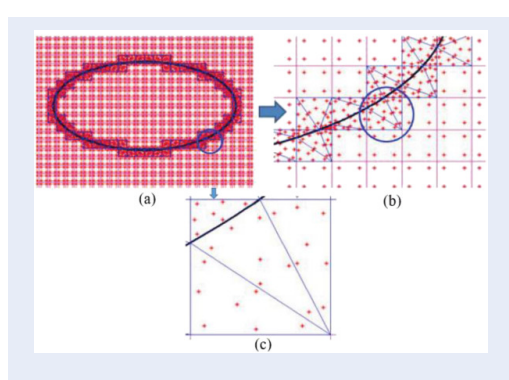


**Figure 2:** Domain subdivision and integration points

In the present work, the mathematical model of the FGM plate problem is based on the **first-order shear deformation theory (FSDT)**. This theory is selected because it accounts for transverse shear deformation effects, which are important in moderately thick plates, while maintaining a relatively simple formulation compared to higher-order theories. The displacement field is therefore expressed in terms of mid-plane displacements and rotations of the normal, with appropriate shear correction factors applied. This choice provides a good balance between

computational efficiency and accuracy for the considered range of plate geometries and thickness ratios.

## **NUMERICAL RESULTS**

## A flat structural slab incorporating voids and fabricated from multifunctional materials, designed to comply with horizontal load-bearing criteria

Let us consider a rectangular flat plate composed of a multifunctional, layered material whose mechanical properties vary along the x-axis within a Cartesian coordinate framework. The plate's geometry and boundary conditions are illustrated in Figure 3. The analysis assumes a plane strain condition. The lower boundary of the plate is fully fixed (clamped). An elliptical void is embedded within the plate, characterized by a major axis of length a and a minor axis of length b. The Poisson's ratio is taken as v=0.3, while the elastic modulus a0 varies according to a prescribed distribution rule described below:

$$E(x) = E_0 e^{\beta x}$$
 with  $E_0 = 10^3$  and  $\beta = 2$ 

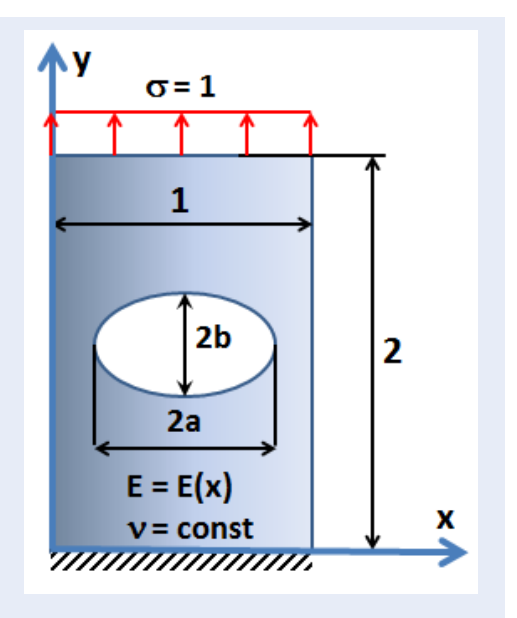


**Figure 3**: A flat plate composed of multifunctional material with properties varying along the horizontal (x) direction

Initially, let us select a=0.27m and b=0.27m, resulting in a circular void within the flat plate composed of functionally layered material. The outcomes obtained using the Extended Finite Element Method (XFEM) will be compared against benchmark results from the Element-Free Galerkin (EFG) method (Figure 4 and Figure 5).

The Element-Free Galerkin (EFG) method was selected as the benchmark because it is a well-established meshfree approach that has demonstrated high accuracy and robustness in problems involving complex geometries, discontinuities, and material inhomogeneities. Its ability to avoid mesh connectivity entirely makes it particularly suitable for modeling plates with arbitrary openings, providing a strong reference for validating the accuracy of the proposed XFEM-based formulation.

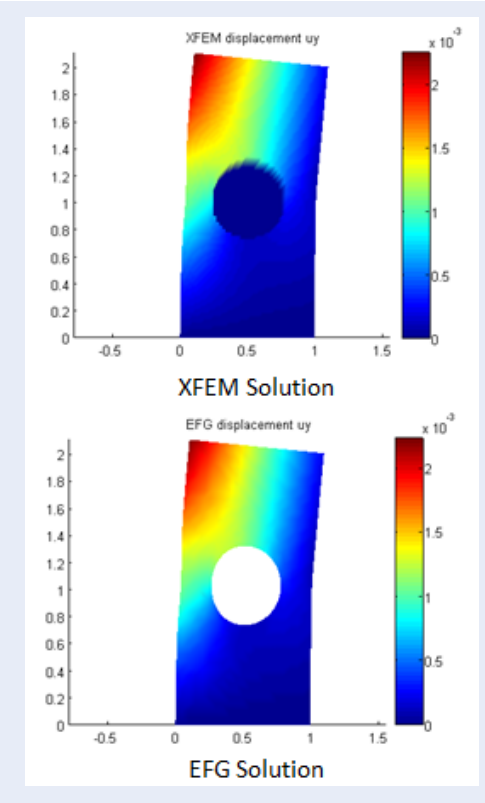


**Figure 4:** Compare the results of the displacement  $u_y$  between XFEM and EFG

Table 1: Comparison of results between XFEM and EFG

	XFEM	EFG	% Error
Max(u <sub>y</sub> )	0.00225	0.00223	0.89%
SCF	6.207	6.188	0.31%

The computational results derived from both the XFEM and EFG methods are presented in Table 1, along with the corresponding percentage errors. It is evident that the stress concentration factor (SCF) and the maximum displacement values obtained using

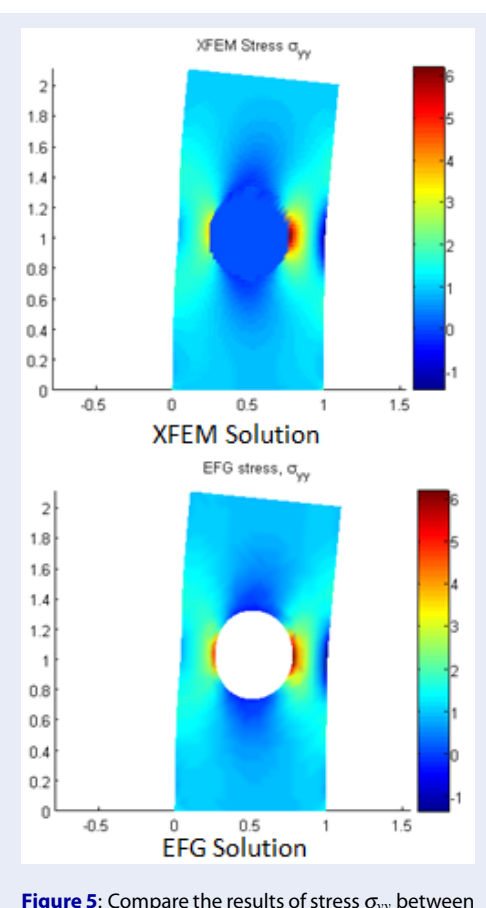


Figure 5: Compare the results of stress  $\sigma_{yy}$  between XFEM and EFG

XFEM closely align with those generated by the meshfree Element-Free Galerkin (EFG) method. The distributions of stress and displacement within the flat plate are illustrated in Figure 4 and Figure 5 . Subsequently, by selecting a=0.26m and b=0.13 m, an elliptical void is introduced into the flat plate composed of functionally layered material. The results obtained from the Extended Finite Element

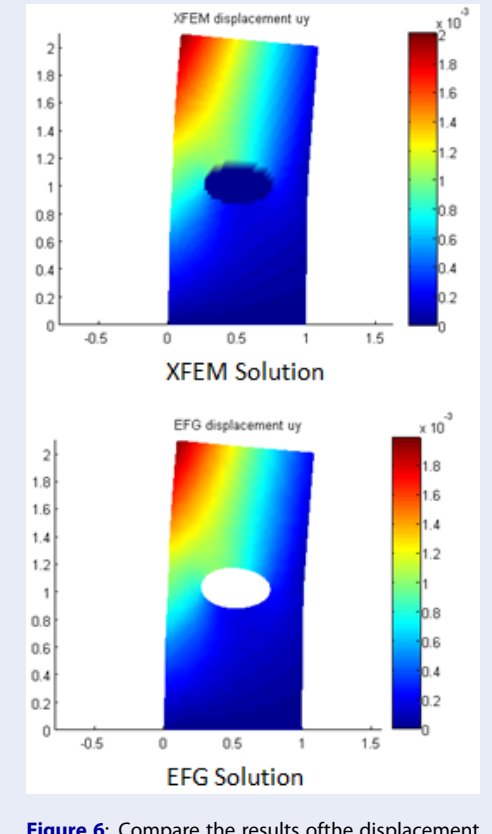
Method (XFEM) will be compared with reference solutions generated by the Element-Free Galerkin

Table 2: Comparison of results between XFEM and EFG

(EFG) method (Figure 6 and Figure 7).

	XFEM	EFG	% Error
Max(u <sub>y</sub> )	0.00200	0.00199	0.50%
SCF	7.300	7.208	1.28%

The stress concentration factor (SCF) and maximum displacement values for the flat plate containing an elliptical void within a functionally layered material are



**Figure 6:** Compare the results of the displacement  $\mathbf{u}_{\mathbf{y}}$  between XFEM and EFG

clearly presented in Table 2 . The results obtained via the Extended Finite Element Method (XFEM) show no discernible deviation from those produced by the mesh-free Element-Free Galerkin (EFG) method. The corresponding stress and displacement fields are illustrated in Figure 6 and Figure 7.

The slightly higher error in the SCF for the elliptical opening (1.28%) is attributed to the increased complexity in capturing the curvature and stress concentration behavior around the elongated boundary. Elliptical geometries produce a more localized and sharper stress gradient near the tips of the major axis compared to circular openings, which poses additional challenges for numerical integration in XFEM. While the level set representation accurately captures the geometry, the enrichment and numerical quadrature in elements intersected by the highly curved boundary can lead to a marginal increase in error. Nevertheless, the error remains within 1.3%, confirming the robustness of the proposed method.

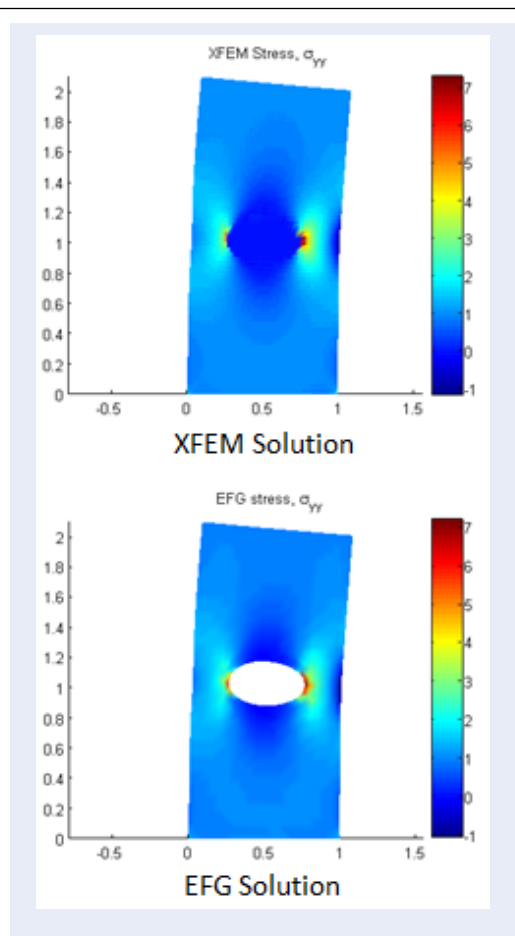


**Figure 7**: Compare the results of stress  $\sigma_{yy}$  between XFEM and EFG

# Flat plate containing round hole with multifunctional material obeys radial law

In the next model, the author will investigate the change of stress concentration factor (SCF) according to the change of the ratio of round hole diameter D to width W of flat plate under the effect of tensile load. Let H=W=5m. The flat plate is made of functional layering material with the law of radial distribution. Given Poisson's ratio v=0.25 and the elastic modulus follows the rule as below (Figure 8):

$$E_{-}(r) = 0.5E_{0} \left( 1 + \frac{e}{e^{r/r_{0}}} \right)$$
  
 $E_{+}(r) = E_{0} \left( 1 - 0.5 \frac{e}{e^{r/r_{0}}} \right)$   
with  $E_{0} = 1000$  and  $r_{0} = D/2$ 

We check the accuracy of the results obtained from XFEM with reference results from the literature  $^{16}$ . The multifunctional material of the flat plate is considered according to the rules  $E_-(r)$  and  $E_+(r)$ . The variation of the stress concentration factor (SCF) with respect to the D/W ratio is shown in Figure 9 and Figure 10.

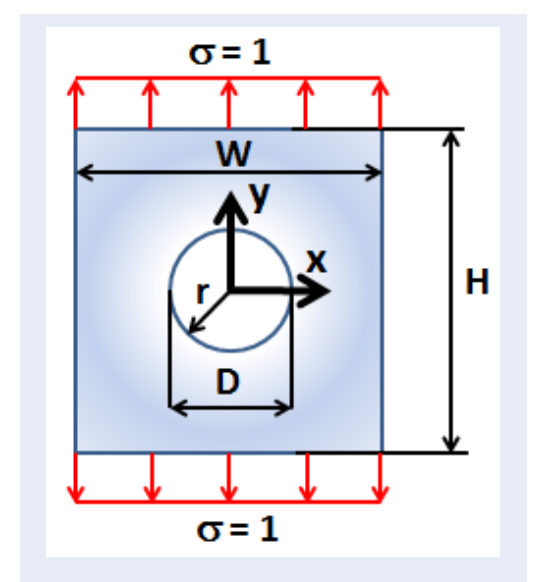


**Figure 8**: Flat plate with multifunctional material distributed according to radial law

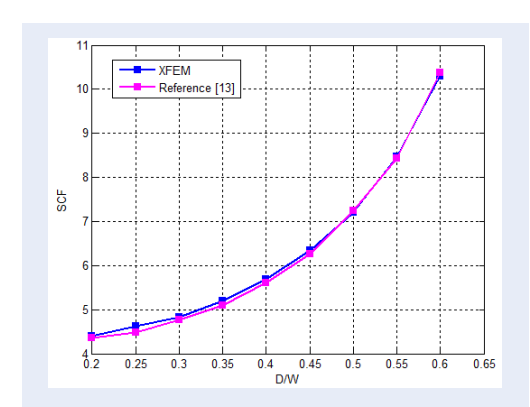


**Figure 9**: SCF in the case of materials obeying the  $E_{-}(r)$  rule

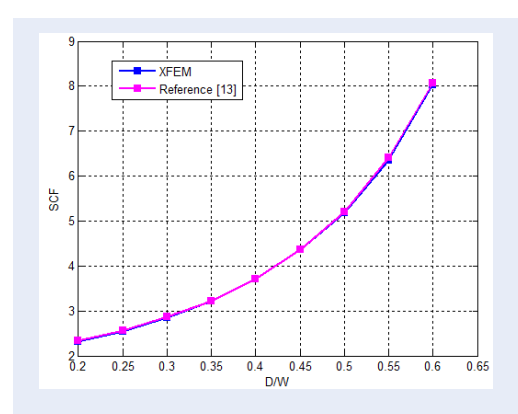


Figure 10: SCF in the case of materials obeying the law  $E_+(\mathbf{r})$ 

In the numerical examples of the present study, the XFEM formulation was implemented using four-node quadrilateral (Q4) finite elements with bilinear shape functions. The number of finite elements in each model depended on the geometry and boundary conditions; for instance, the plate with a circular opening was discretized into  $120\times120120$  \times  $120120\times120$  elements, while the plate with an elliptical opening used  $140\times140140$  \times  $140140\times140$  elements to better capture the curved boundary. The enrichment zone included all elements intersected by the hole boundary and their immediate neighbors.

For the comparison method, the Element-Free Galerkin (EFG) approach was implemented with cubic spline weight functions and a support domain size of 3.0 times the nodal spacing. The EFG domain was discretized using a uniform nodal distribution matching the XFEM resolution to ensure a fair comparison of accuracy and computational cost.

## Let us consider a plate containing a concentric circular hole. The parameters of the problem are as follows: (Figure 11)

 $E = 210000N/mm^2$ ; v = 0.3; l = 200mm; a = 10mm; w = 100mm = 2b; t = 10m,  $\sigma_0 = 100M/mm^2$ 

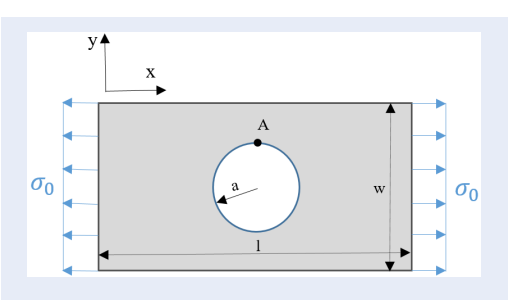


**Figure 11**: Round hole in a thin plate subjected to uniaxial uniform tensile load

According to analytic theory, we have proved that the maximum stress is obtained at point A, we have:

$$(\sigma_{\theta}) = 3\sigma_0 = 300 \, N/mm^2$$

Stress concentration factor at A:

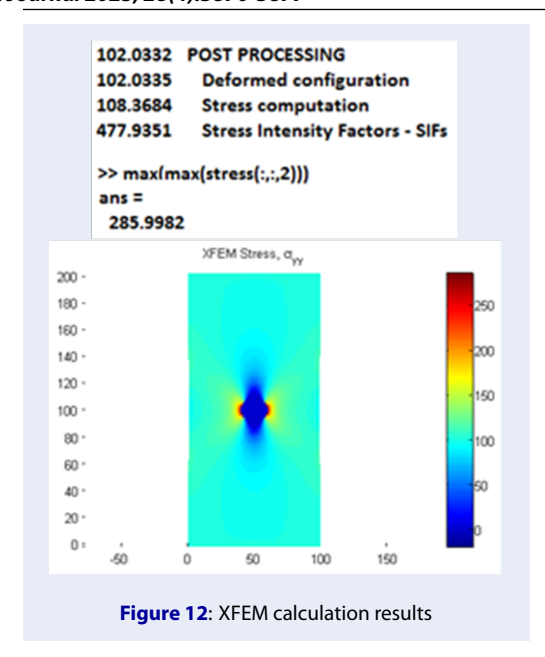
$$K_t = \frac{\sigma_{max}}{\sigma_0} = 3$$

XFEM calculation results (Figure 11):

$$K_{tXFEM} = \frac{\sigma_{max}}{\sigma_0} = \frac{285,9982}{100} = 2,86$$

Error

$$K_{tXFEM} = \frac{K_t - K_{tXFEM}}{K_t} . 100\% = \frac{285,9982}{100} = 4,67 < 5\%$$



## **CONCLUSIONS**

In this chapter, various examples of the applications of the XFEM have been shown. These examples demonstrate that XFEM is advantageous in modeling discontinuities such as holes and inclusions.

Section 3.1. shows XFEM is very good when compared with EFG methods. The calculation results obtained from XFEM and EFG are listed in Table 1, including % error. It can be seen that the stress concentration factor (SCF) and the maximum displacements possible obtained from XFEM are not significantly different from those obtained from EFG. The stress and displacement fields of the flat plate are shown in Figure 4 and Figure 5 As we can see, the % error is fully listed in Table 2. Both numerical methods give fairly similar results. The stress and displacement fields of the flat plate are shown in Figure 6 and Figure 7. In section 3.2, We can see that the stress concentration factor (SCF) obtained from the XFEM calculation program is quite similar to the reference results from <sup>16</sup>. In future work, the proposed XFEM-level set framework could be extended to three-dimensional FGM structures and applied to investigate the interaction effects between multiple openings and cracks.

## **ABBREVIATIONS**

XFEM: Extended Finite Element Method SCF: Stress concentration factor

# AVAILABILITY OF DATA AND MATERIALS

The data and materials used and/or analyzed during the current study are available from the corresponding author upon reasonable request.

# ETHICS APPROVAL AND CONSENT TO PARTICIPATE

Not applicable.

## **CONSENT FOR PUBLICATION**

Not applicable.

## **COMPETING INTERESTS**

The author declares that they have no competing interests.

## **AUTHORS' CONTRIBUTIONS**

Conceptualization, H.-D.N.; methodology, H.-D.N.; software, H.-D.N.; validation, H.-D.N.; formal analysis, H.-D.N.; investigation; resources, H.-D.N.; data curation, H.-D.N.; writing—original draft preparation, data curation; writing—review and editing, data curation; supervision. The author read and agreed to the published version of the manuscript.

## **ACKNOWLEDGEMENTS**

The author would like to thank DLA for supporting this article.

## **REFERENCES**

- Krishnamoorthy CS. Finite element analysis Theory and Programming. New Delhi: Tata McGraw-Hill; 1997.
- Huynh DBP, Belytschko T. The extended finite element method for fracture in composite materials. International Journal For Numerical Methods in Engineering. 2008;
- Nguyen HD. Using Matlab to Study of the Response of the System to Oscillatory Influences be an Oscillatory Effect on the Resting Antenna. Int J Multidiscip Res Growth Eval. 2025;27:885.
- Nguyen HD. Application of the Extended Finite Element Method (X-FEM) for Simulating Random Holes in Functionally Graded Plates. International Journal of All Research Writing. 2025;6(12).
- Daux C, Moes N, Dolbow J, Sukumar N, Belytschko T. Arbitrary cracks and holes with the extended finite element method. Int J Numer Methods Engrg. 2000;48(12):1741–1760.
- Nguyen HD. Using the eXtended Finite Element Method (XFEM) to Simulate Own Frequency under External Influences of a Closed System based on Dynamic Compensation Method. J Int Multidiscip Res. 2025;27(7):985.
- Dolbow J, Moes N, Belytschko T. Modelling fracture in mindlinreissner plates with the extended finite element method. Int J Solids Struct. 2000;37(48-50):7161–83.
- Nguyen HD. Extended Finite Element Approach for Simulating Arbitrary Openings in Functionally Graded Plates. Int J Mech Energy Eng Appl Sci. 2025;.
- Nguyen HD. Using Finite Element Method to Calculate Strain Energy Release Rate, Stress Intensity Factor and Crack Propagation of an FGM Plate Based on Energy Methods. Int J Mech Energy Eng Appl Sci. 2025;17(2):10345.

- Nguyen HD, Huang SC. Calculating Strain Energy Release Rate, Stress Intensity Factor and Crack Propagation of an FGM Plate by Finite Element Method Based on Energy Methods. Materials (Basel). 2025;18(12):2698. Available from: http://doi. org/10.3390/ma18122698.
- Nguyen HD, Huang SC. Designing and Calculating the Nonlinear Elastic Characteristic of Longitudinal–Transverse Transducers of an Ultrasonic Medical Instrument Based on the Method of Successive Loadings. Materials. 2022;15(11):4002.
- Nguyen HD, Huang SC. The Uniaxial Stress Strain Relationship of Hyperelastic Material Models of Rubber Cracks in the Platens of Papermaking Machines Based on Nonlinear Strain and Stress Measurements with the Finite Element Method. Materials. 2021;14(24):7524.
- 13. Nguyen HD, Huang SC. Using the Extended Finite Element Method to Integrate the Level-Set Method to Simulate the

- Stress Concentration Factor at the Circular Holes Near the Material Boundary of a Functionally-Graded Material Plate. JMR&T. 2022;21C:4658–4673.
- Nguyen HD, Huang SC. Use of XTFEM based on the consecutive interpolation procedure of quadrilateral element to calculate J-integral and SIFs of an FGM plate. Theor Appl Fract Mech. 2023;127. Available from: http://doi.org/10.1016/j.tafmec.2023.103985.
- Nguyen HD, Huang SC. Applying Quarter-Point Singular Element in Finite Element Method to Calculate J-Integral and Stress Intensity Factors of a Rectangular Isotropic FGM Plate. A S . 2025;.
- Yang Q, Gao C, Chen W. Stress concentration in a finite functionally graded material plate. Sci China-Phys Mech Astron. 2012;55:1263–1271. Available from: http://doi.org/10.1007/s11433-012-4774-x.